ELSEVIER

Journal of Chromatography B, 754 (2001) 11–21

JOURNAL OF CHROMATOGRAPHY B

www.elsevier.com/locate/chromb

Experimental design methodology applied to the study of channel dimensions on the elution of red blood cells in gravitational field flow fractionation

Sousan Rasouli, Emmanuel Assidjo, Thierry Chianéa, Philippe J.P. Cardot*

Laboratoire de Chimie Analytique et de Bromatologie, Université de Limoges Faculté de Pharmacie, 2 Rue du Dr. Marcland, F-87025 Limoges Cedex, France

Received 20 December 1999; received in revised form 7 September 2000; accepted 3 November 2000

Abstract

Field flow fractionation (FFF) separation techniques have gained considerable success with micron-sized species. Living red blood cells (RBCs) of any origin have emerged as ideal models for cell separation development. Their elution mode is now described as ''Lift-Hyperlayer''. Certain separator dimension parameters are known to play a key role in the separation and band spreading process. Systematic studies of channel dimensions effects on RBC retention, band spreading, peak capacity and on a novel parameter described as ''Particle Selectivity'' were set up by means of a two-level factorial experimental design. From experimental results and statistical calculations it is confirmed that channel thickness plays a major role in retention ratio, peak variance, peak capacity and particle selectivity. Channel breadth strongly influences plate height, with lower impact on peak capacity and particle selectivity. Retention ratio, peak variance and peak capacity observed results are modulated by second-order interactions between channel dimensions. Preliminary rules for channel configurations are therefore set up and depend on separation goals. It is shown that a very polydisperse population is best disentangled in a thin and narrow channel whatever its length. If a mixture of many different micron-sized species is considered (each of limited polydispersities); a thick and broad channel should be preferred, with length modulating peak capacity to disentangle this polymodal mixture.

Keywords: Channel dimensions; Red blood cells; Gravitational field-flow fractionation

1. Introduction

Field flow fractionation (FFF) is a family of separation techniques applicable to the separation and characterisation of macromolecular, colloidal and micro-particulate species whose size ranges from 10^{-3} to 10^{2} μm [1,2]. This technique was introduced in 1966 by Giddings [3] and its general principle is now well-established [4–9]. Sedimentation FFF (SdFFF) that uses either centrifugal force (multi-gravitational FFF) or merely earth gravity (G-FFF) to operate, gained considerable success in the separation and purification of micron-sized species of biological origin, where the red blood cell (RBC) emerged as an ideal model [10–12].

The elution of micron-sized species of any origin in SdFFF is described by the ''Lift-Hyperlayer'' model [4] in which it is assumed that no attractive or

*Corresponding author. Tel.: +33-5-5543-5857; fax: +33-5-5543-5859.

E-mail address: cardot@unilim.fr (P.J.P. Cardot).

0378-4347/01/$ – see front matter
PII: S0378-4347(00)00581-8

repulsive particle–wall interactions occurred. In this model, during elution, the micron-sized species are submitted to the balance of two opposite forces: one produced by the external field and the second, of hydrodynamic origin, described as ''lift forces'' [13]. Such interactions focus the particles into an equilibrium position in the channel thickness, according either to particle characteristics like size and density [7], either to the operating conditions like external field intensity and flow velocity [14–16].

The ''Lift-Hyperlayer'' elution process is now well-established for mono and polydisperse micron-sized species, such as latex [17], silica [18] and RBCs [11]. In the following work, it is assumed that the ''Steric'' elution mode is a limit condition of the ''Lift-Hyperlayer'' model when lift forces effects are reduced by the external field, to a negligible extent. This, led to particle retention being size dependent and independent of flow velocity.

Much information can be obtained from an eluted peak profile, they are: the retention ratio which is related to the particle mean characteristics; the band spreading which is a indirect probe of sample polydispersity and the peak capacity defined as the maximum number of separable peaks [19].

In the present work, we describe the particle selectivity (P.S.), a probe of the separator capacity to disentangle the different constituents of a polydisperse sample. It has roots in the hypothesis that, in the ''Lift-Hyperlayer'' mode, retention ratio is related to a particle average equilibrium position x_{eq} as already described by Williams et al. [13]. This equilibrium position, in the channel thickness, is calculated from retention ratio by means of Eq. (1):

$$R = 6 \cdot \frac{x_{eq}}{w} \cdot \left(1 - \frac{x_{eq}}{w}\right) \quad (1)$$

with w being the channel thickness. For a given channel and a given polydisperse sample, retention ratios of the eluted peak profile front (R_1) and tail (R_2) correspond to the respective positions $x_{eq1}$and x_{eq2} shown in Fig. 1. P.S. is related to channel thickness and effective separation length by Eq. (2):

$$\text{P.S.} = \frac{(\Delta x_{eq})/w}{(L - l)} \quad (2)$$

with, $\Delta x_{eq} = x_{eq2} - x_{eq1}$, L the channel length and l the length occupied by the injection volume.

However, peak profile characteristics are affected by channel dimensions and experimental conditions, i.e., concentration, injection volume, flow velocity and stop-flow procedure [14,20–22]. Consequently, for a given sample and experimental conditions, the effects of the channel dimensions on the peak characteristics are investigated studying RBC elutions. Two different separation objectives have to be achieved in FFF. First the separation of sub-populations of a polydisperse sample, second the separation from a mixture composed of a large number of different monodisperse populations. Reports studying some aspects of the channel dimensions are available with latex particles and RBCs [14,23–25]. However, none described any possible dimension interactions. In that purpose, the most simple sedimentation FFF technique (G-FFF) associated to an experimental design methodology were set up to determine channel dimension effects on RBC retention and band spreading characteristics.

2. Statistical methodology

A two-level factorial experimental design [26] studying each factor, i.e., channel dimensions at two levels (low level coded by -1 and high level coded by $+1$) was used. The channel set up was therefore, limited to 2^k (k being the number of factors involved, in this report $k=3$).

Channel breadth (x_1), thickness (x_2) and length (x_3) are the studied factors and the system response (y_i) may be either particle selectivity, peak capacity or retention ratio, either peak variance and plate height.

Coefficients a_1, a_2 and a_3 were associated to each factor (principal coefficients) and a_1a_2, a_1a_3, a_2a_3 and $a_1a_2a_3$ to their interactions with the other parameters (interaction coefficients). These coefficients whose values describe the influence of the corresponding factor on the system are calculated using the following equation:

$$a_i = \frac{\sum_{j=1}^{N} y_{i+} - \sum_{j=1}^{N} y_{i-}}{N} \quad (3)$$

where Σy_{i+} and Σy_{i-} represent, respectively the sum

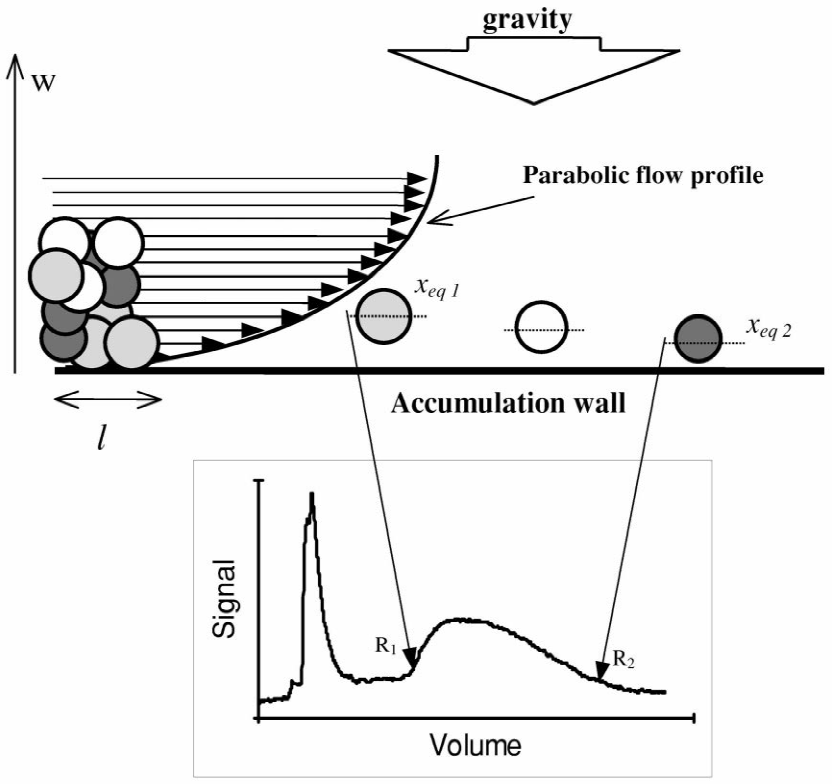

Fig. 1. ''Lift-Hyperlayer'' elution mode of polydisperse sample. Upper: parabolic flow profile of the carrier phase in the channel thickness. Right polydisperse sample at injection. Left: equilibrium position of the different sub populations. x_{eq1} and x_{eq2} correspond, respectively, to an equilibrium position in the channel thickness of the subpopulations the less and the more retained. Lower: x_{eq1} and x_{eq2} equilibrium positions calculated from retention ratio and used for particle selectivity calculations. x_{eq1} and x_{eq2} are calculated using Eq. (1).

of the response for high and low levels and N is the number of experiments. Table 1 presents a schematic model of Σy_{i+} and Σy_{i-} calculation for each coefficient.

For each system response a single experimental standard deviation (Se) was calculated as described in the literature [26]. If an absolute value of a principal coefficient (a_i) is superior to twice the experimental standard deviation ($a_i > 2\mathrm{Se}$), then the corresponding factor influences the system response. The higher this value, the more important the influence.

The negative sign of a principal coefficient (a_i) predicts relatively high values of system response for a low level of the studied parameter

In order to take into consideration an interaction coefficient, the value of $a_i a_j$ and those of the involved parameters (a_i and a_j) must also be superior to 2Se. In that case, a positive sign of the coefficient predicts a higher intensity of the interaction effect for the identical sign of the parameters involved [high ($+1$) and high ($+1$) level or low (-1) and low (-1) level].

3. Experimental

3.1. Experimental design in G-FFF

A two-level factorial experimental design was applied. A combination of low and high levels of three factors (channel breadth, thickness and length)

Table 1
Statistical experimental design model for y_{i+} and y_{i-} calculation[a]

	x_0[b] a_0	x_1 a_1	x_2 a_2	x_3 a_3	x_1x_2 a_1a_2	x_1x_3 a_1a_3	x_2x_3 a_2a_3	$x_1x_2x_3$ $a_1a_2a_3$
y_i for channel 1	+1	−1	−1	−1	+1	+1	+1	−1
y_i for channel 2	+1	+1	−1	−1	−1	−1	+1	+1
y_i for channel 3	+1	−1	+1	−1	−1	+1	−1	+1
y_i for channel 4	+1	+1	+1	−1	+1	−1	−1	−1
y_i for channel 5	+1	−1	−1	+1	+1	−1	−1	+1
y_i for channel 6	+1	+1	−1	+1	−1	+1	−1	−1
y_i for channel 7	+1	−1	+1	+1	−1	−1	+1	−1
y_i for channel 8	+1	+1	+1	+1	+1	+1	+1	+1

[a] a_1, a_2 and a_3 are the principal coefficients of channel breadth, thickness and length and a_1a_2, a_1a_3, a_2a_3 and $a_1a_2a_3$ are the interaction coefficients of the corresponding factors

[b] x_0 and a_0 concern the average system response for all experiments.

led to the construction of eight channels whose characteristics are given in Table 2. For each channel, RBC elution was performed and the different system responses were calculated from elution peak characteristics.

3.2. Sample and apparatus

Human blood was drawn from a volunteer after informed consent. Sample storage and dilution have been already described [27] as well as the general set up procedure of the G-FFF channels, volume measurement techniques, and elution methodology [27,28]. Connection and detection volumes are kept constant at 50 μl whatever the channel under consideration. Internal diameter tubing was chosen to minimise the connection volume in correlation with the separator pressure drop (leakage risk).

Table 2
Statistical experimental channels set up[a]

Channel	Breadth (cm)	Thickness (μm)	Length (cm)	Volume (ml)
1	1	100	20	0.26
2	2	100	20	0.45
3	1	250	20	0.53
4	2	250	20	1.05
5	1	100	50	0.56
6	2	100	50	1.04
7	1	250	50	1.31
8	2	250	50	2.59

[a] Connection and detection volumes are kept constant at 50 μl whatever the separator under consideration.

3.3. Set up of the experimental conditions

For data analysis, experiments must be carried out under identical conditions [26], i.e., sample concentration, injection volume and flow velocity. Previous studies demonstrated the effects of these conditions on the elution characteristics for RBCs [14,27]. A preliminary study was needed that aimed at an optimisation of the experimental conditions in which a maximum of peak retention and a minimum of overloading phenomena were observed for each channel. High sample concentrations are known to affect strongly overloading and band spreading [7,20], consequently diluted samples injections were desired. On the other hand, the detection limit of the UV detector reduced the use of very diluted samples. Therefore, a series of experiments was performed to determine the maximum of injection volume of a diluted sample without significant distortion of peak characteristics. In that objective, a constant quantity of cells ($4.5 \cdot 10^4$ cells/μl, corresponding to a pure blood dilution factor of 100) was injected into the channels at different injection volumes (10 to 100 μl for 20 cm channels and 10 to 200 μl for 50 cm channels). Flow velocity and stop-flow time were fixed at 0.167 cm/s and 2 min. Fractograms obtained with channel 6, one of the two smallest channel volume are shown in Fig. 2.

Elution peak overloading is clearly demonstrated with the more concentrated sample.

To assess the impact of injection volume and sample concentration of elution patterns, systematic study were performed. Data series of Fig. 3 present

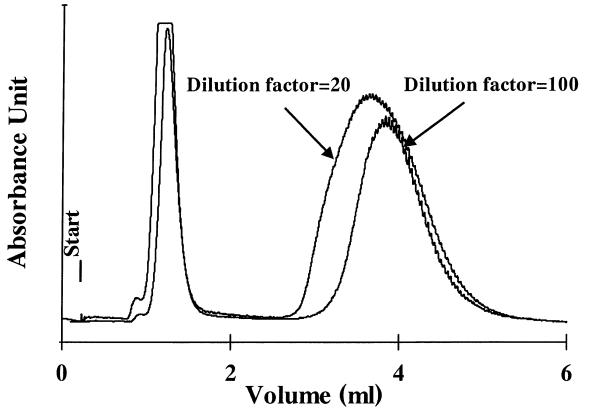

Fig. 2. Evidence of sample overloading on red blood cells fractograms. Flow velocity: 0.167 cm/s, stop flow time 2 min, 25-μl injection loop. Dilution factor 20: $2.25 \cdot 10^5$ cell/μl and 100: $4.5 \cdot 10^3$ cell/μl. Signal scale intensities are normalised for peak profile comparison (scale ratio = 4).

the peak characteristics patterns for channels 1, 2, 5 and 6. It appeared that retention ratio increases as injection volume increases. Similar dependence was observed for all of the other channels. Asymmetry factor behaviour was different for 20 cm and 50 cm channels whereas HETP decreases as injection volume increase for any channel.

A combination of peak characteristics results for all channels led to the use of a 25 μl injection volume. This volume, being the limiting one as shown for the retention ratio and asymmetry factor behaviour of Fig. 3.

In order to control the choice of the initial sample concentration a series of experiments was performed using dilution factors varying from 4 to 1000 (injected concentrations varied from $1.12 \cdot 10^6$ to $4.5 \cdot 10^3$ cells/μl) as described by Assidjo and Cardot [27]. A 25-μl injection loop, flow velocity of 0.167 cm/s and stop-flow time of 2 min was applied. Results shown in Fig. 4 data series for channels 1, 2, 5 and 6 demonstrated that elution peak characteristics decreased systematically as dilution factor increased. A chemometric method (analysis of variance, ANOVA) [29] was used to determine the limit corresponding to the minimal dilution factor associated with constant peak characteristics. It appeared that the minimal dilution factor obtained for all types of channels was 100 confirming the choice of the initial sample concentration.

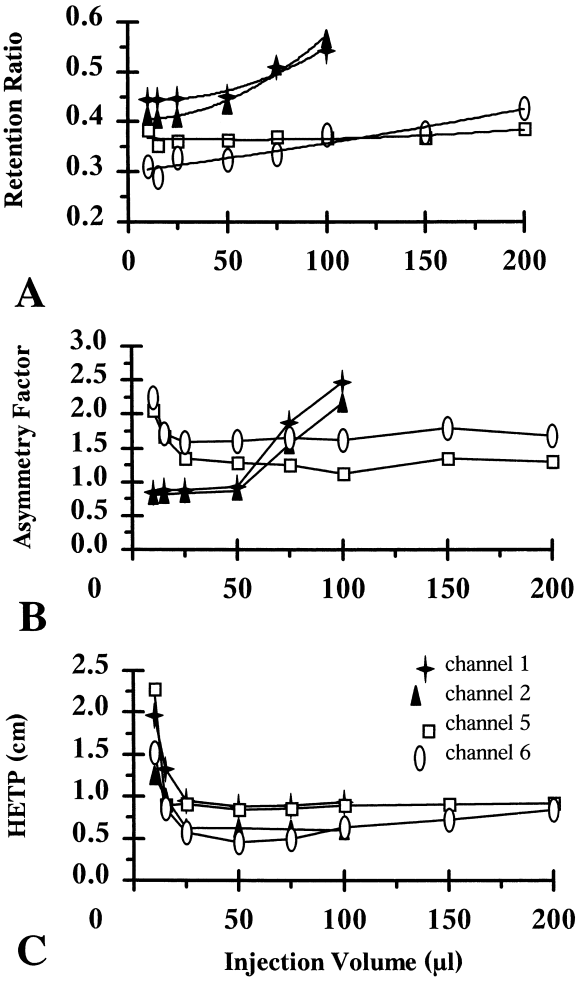

Fig. 3. Peak characteristics optimisation for channels 1, 2, 5 and 6. (A) Retention ratio, (B) asymmetry factor and (C) HETP. Injection volume varies from 10 to 100 μl for channels 1 and 2 and from 10 to 200 μl for channel 5 and 6, flow velocity 0.167 cm/s, stop flow time 2 min, $4.5 \cdot 10^4$ red blood cells injected. Channels 1 and 2 are those of smallest void volume, while channels 5 and 6 are those of intermediate ones.

4. Results and discussion

4.1. Elution mode

The ''Lift-Hyperlayer'' elution mode is flow velocity dependent [4]. It is therefore necessary to verify that such a model can be applied to any of the channel dimensions involved in this study. For this purpose, RBC elutions were performed at different

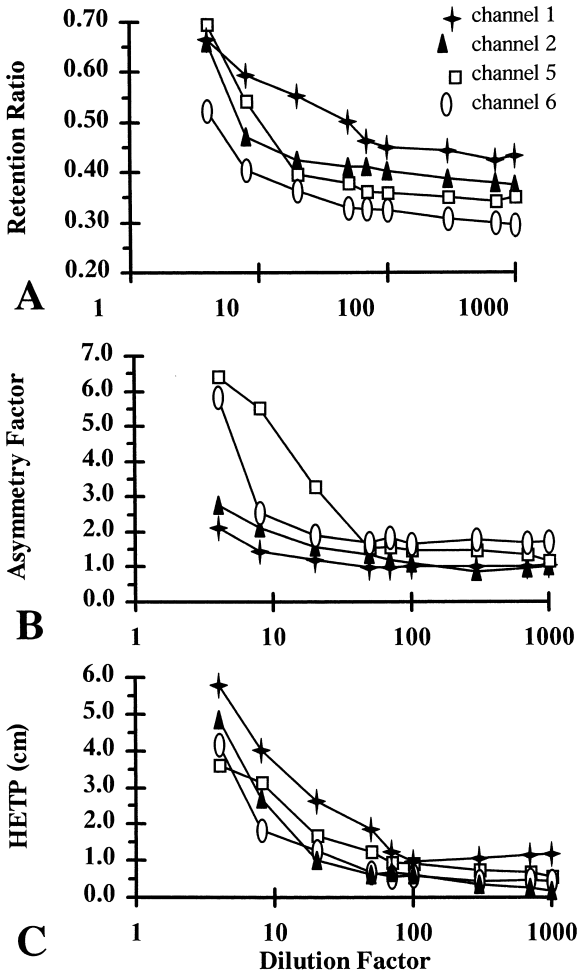

Fig. 4. Sample concentration effects on elution peak characteristics for channels 1, 2, 5 and 6. (A) Retention ratio, (B) asymmetry factor and (C) HETP. Dilution factor varies from 4 to 1000, flow velocity 0.167 cm/s, stop flow time 2 min, 25 μl injection loop.

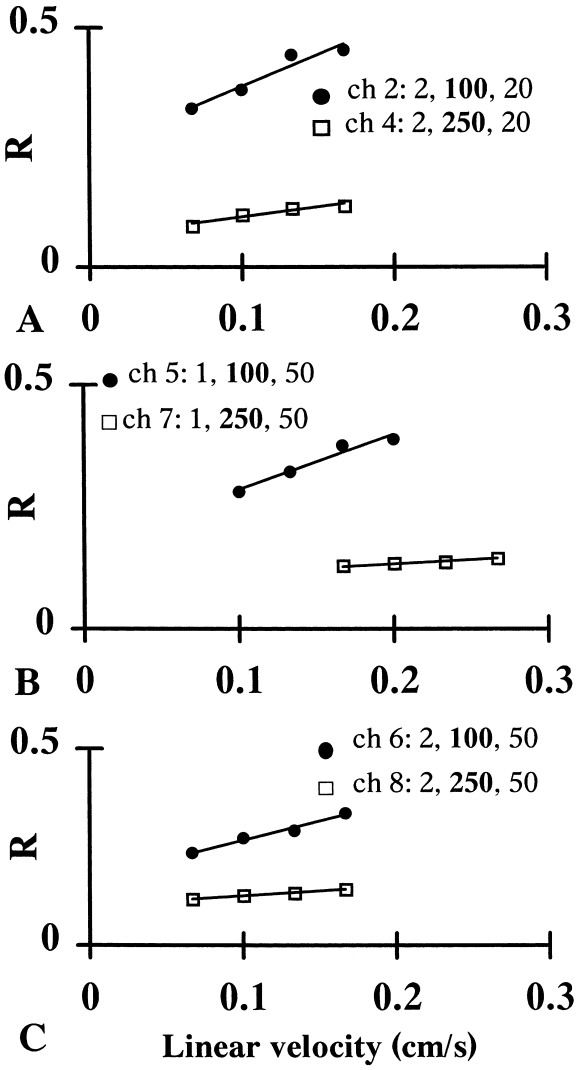

Fig. 5. Effects of channel thickness on RBC retention ratio. Elution conditions are: flow-rate 0.167 cm/s, 25 μl injection loop, $4.5 \cdot 10^4$ red blood cells injected, stop flow time 2 min. Channel characteristics as described in Fig. 4.

flow velocities for every channel. The retention ratios obtained were plotted versus linear velocities, as shown in the series of Figs. 5–7, corresponding, respectively, to channel thickness, length and breadth. These data demonstrate that the retention ratio increased when the flow velocity increased, a general characteristic of the ''Lift-Hyperlayer'' elution mode.

When channel thickness was considered, as shown in Fig. 5, it was observed that RBCs were systematically more retained in the thicker channels. For similar average flow velocity increments, the lifting forces acting on the RBCs were systematically greater in the thinner channels as demonstrated by the retention ratio slope differences. The greater the slope, the stronger the lifting forces.

Considering the other channel dimensions which are length and breadth, no mode dependent conclusions were provided for the ''Lift-Hyperlayer'' elu-

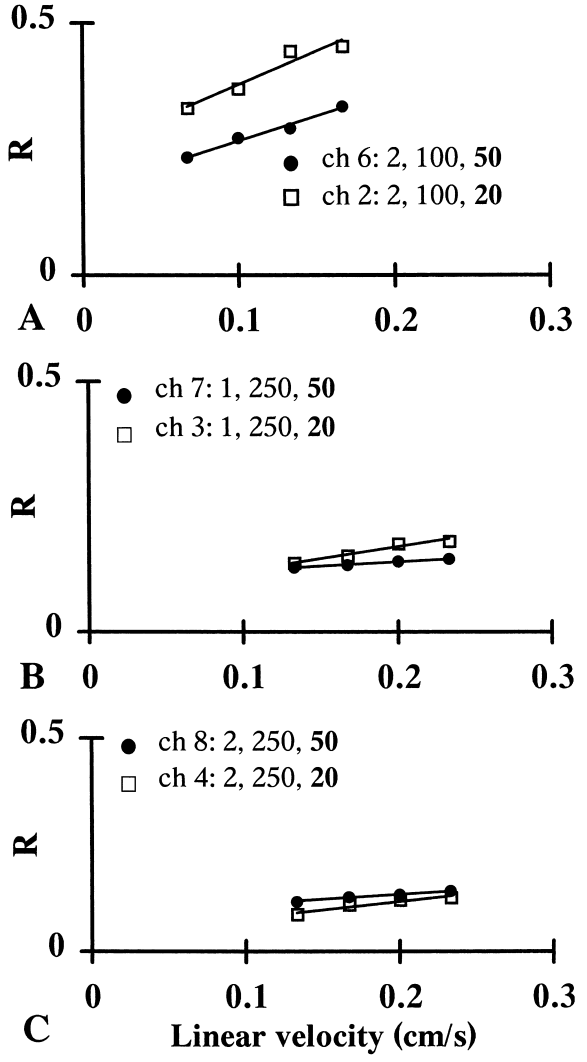

Fig. 6. Effects of channel length on RBC retention ratio. Conditions as described in Fig. 4.

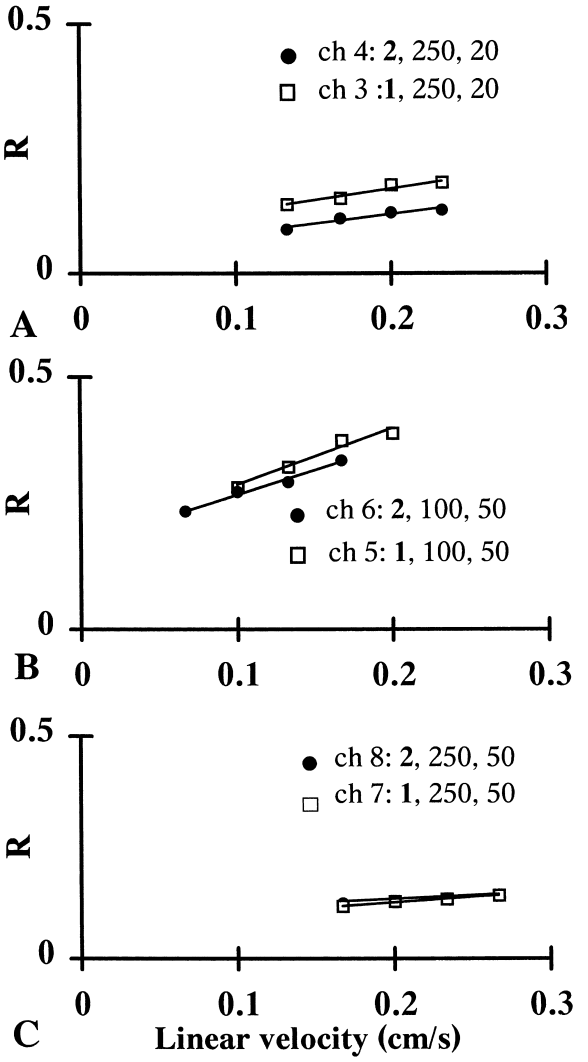

Fig. 7. Effects of channel breadth on RBC retention ratio. Conditions as described in Fig. 4.

tion mode. This hypothesis was confirmed experimentally by the results of Figs. 5 and 6 from which no general rules emerge. Thus, a complete statistical data analysis was required.

4.2. Experimental results and statistical interpretations

Table 3 presents two groups of the experimental system responses, obtained for every channel. The first group concerns classical elution probes, which are retention ratio (R), peak variance (σ_{vol}) and plate height (H). The second includes peak capacity (n) and particle selectivity (P.S.). Using Eq. (3) and the data of Tables 1 and 3, the principal coefficients (a_1, a_2 and a_3) and interaction coefficients (a_1a_2, a_1a_3, a_2a_3 and $a_1a_2a_3$) were calculated and results are listed in Table 4. The randomised experimental standard deviations (Se) were calculated using data from channels 8, 3, 4, 1 and 7 for five system

Table 3
System responses values of the statistical experimental design[a]

Channel	R	σ_{vol} (ml)	H (cm)	n	P.S. ($\cdot 10^{-5}$)
1	0.440	0.37	0.952	2.88	316
2	0.418	0.61	0.613	3.11	257
3	0.171	1.71	0.903	3.65	98.1
4	0.155	2.88	0.518	5.09	53.1
5	0.363	0.74	0.909	3.84	293
6	0.329	0.85	0.571	4.63	221
7	0.143	2.52	0.756	6.75	69.1
8	0.129	3.13	0.335	8.14	38.4

[a] Conditions as described in Fig. 4.

responses, respectively [26] and results are presented in Table 5.

4.2.1. Retention ratio

The high value of a_2 (the principal coefficient of the channel thickness) relative to Se, demonstrates a great influence of this channel dimension on the retention ratio ($|0.19| \gg 0.008$) as shown in Table 2. Each of the two other coefficients under study (a_1, a_3) were of much lower absolute values, which led to the conclusion that the corresponding channel dimensions (i.e., breadth and length) did not influence the retention ratio significantly.

The negative sign associated with coefficient a_2 means that relatively high values of R are expected when this parameter is at its low level (in that case 100 μm). This interpretation was confirmed by Table 3 data and in agreement with Fig. 3 results. As for channel breadth and length, the negative sign of the corresponding coefficients predict that the retention ratio values must be relatively higher when these parameters are at their low levels and again this is confirmed by Table 3 data.

A moderate value of coefficient a_2a_3 was observed, showing the possible interaction between channel thickness and length. Its positive sign predicted an effect of this interaction for the identical criteria of these channels dimensions (100 μm, 20 cm or 250 μm, 50 cm). As a consequence of this interaction, the results shown in Table 3 demonstrate higher values of R for channels 1 and 2 in comparison with channels 5 and 6.

Table 5
Calculated experimental standard deviations, using channels 8, 3, 4, 1 and 7 for all system responses

	R	σ_{vol}	H	n	P.S. ($\cdot 10^{-5}$)
Se	0.004	0.064	0.017	0.118	4.8
2Se	0.008	0.128	0.034	0.236	9.6

4.2.2. Peak variance

Peak variance studies underlined a major influence of the channel thickness, as shown by the high value of the corresponding coefficient a_2 of Table 4, relative to Se ($|0.959| \gg 0.128$). This channel dimension can be considered as a first-order parameter. The impact of the channel breadth and length on this system response is significantly less important, as the absolute values of their coefficients are only moderately superior to 2Se. The positive sign of coefficient a_2 predicts relatively high values of peak variance for the thicker channels, as shown by Table 3 data for 250 μm channels. The two other principal coefficients (a_1 and a_3) were positive and led to the prediction that higher peak variance may be expected for broader and longer channels (in comparison with the narrower and shorter ones). However, Table 3 data shows two abnormalities. The first one is linked to channel 3 where σ_{vol} was significantly lower than that of channels 4, 7 and 8 (all being thick channel). The second abnormality raised from channels 3 and

Table 4
Principal and interaction coefficients calculated from Eq. (3) and data in Tables 1 and 3 for all system responses[a]

	a_0	a_1	a_2	a_3	a_1a_2	a_1a_3	a_2a_3	$a_1a_2a_3$
R	0.269	−0.011	−0.119	−0.028	0.003	−0.001	0.014	0.002
σ_{vol}	1.601	0.266	0.959	0.209	0.179	−0.086	0.056	−0.054
H	0.695	−0.185	−0.067	−0.052	−0.016	−0.004	−0.030	−0.005
n	4.761	0.481	1.146	1.079	0.226	0.064	0.459	−0.076
P.S. ($\cdot 10^{-5}$)	168	−26	−104	−13	6.91	0.16	1.91	3.41

[a] Conditions as described in Fig. 4.

4 compared to channels 7 and 8. In these cases, a peak variance increase was predicted due to the effect of channel breadth. This increase was much lower when channels 7 and 8 were compared to channels 3 and 4. These two anomalies were explained by an interaction between channel breadth and thickness as shown by the value of coefficient a_1a_2 of Table 4.

4.2.3. Plate height

Contrary to the two previous response systems, the data displayed in Table 4 show a much weaker impact of channel thickness on plate height value. The first-order parameter in this system response appeared to be the channel breadth as confirmed by the absolute value of the linked principal coefficient ($|0.185| \gg 0.034$). However, channel length and thickness played a second-order role. By analogy from the peak variance study, it can be concluded that thickness played a more important role than length. Again, the negative sign allows the prediction that higher H values would be obtained for the low levels of the corresponding channel dimensions. Table 4 interaction data lead to the conclusion that no significant channel dimension interactions occurred.

4.2.4. Peak capacity

In that system response, two channel dimensions played a first-order role, i.e., channel thickness and length. Channel breadth played a significant second-order role. The systematic positive sign of all the principal coefficients predicts an increased peak capacity for thicker and longer channels, the positive sign of a_1 shows that an increase of peak capacity was also expected for broader channels. All this statistical information is qualitatively confirmed by Table 3 data. An interaction diagnosed between channel thickness and length was shown by the absolute value of coefficient a_2a_3. According to the interpretation rules, this interaction occurs when channel thickness and length criteria are identical (100 μm and 20 cm or 250 μm and 50 cm). However, it was difficult to formalise the effects of this interaction on the system response from data in the Table 3.

4.2.5. Particle selectivity

Let us consider the multipolydispersity [30] pattern of a RBC population, these are average values and dispersities among the very different cell characteristics; i.e., size, density and shape. FFF elutions drive systematically to a single fractogram peak with fractions of different characteristics [31]. The separation goal is therefore to obtain fractions of different characteristics within the elution peak. To be able to collect and characterise the maximum number of fractions, fractograms must be as broad as possible. Low retention ratio nor high peak capacity are required. The immediate consequence is that a thin channel must be set up at first intention, as driven by the increased flow profile selectivity as well as the increased particle selectivity showed by the negative sign of a_2 coefficient. The experimental design set up in this report gives additional recommendations. Channel breadth and length have been demonstrated to play a second order role, while no significant interactions emerged from Table 4 data.

With a channel thickness chosen, the second dimension to set up is its breadth, finally the length is to be chosen to allow a channel void volume compatible with the sample volume. Such a channel set up strategy is demonstrated from the experimental design data. Experimental design data of Table 4 showed that particle selectivity was only thickness dependent, whatever the channel length. This result take roots from the complex combination of Δx_{eq} and the effective channel length ($L-l$). The absence of interactions between particle selectivity and channel length is of interesting consequences. First, relatively large injection volumes can be used, second miniaturised G-FFF channels can be set up. For practical applications $125-80$ μm thickness are recommended, with breadth in the 0.5 to 2 cm range and minimum length of 20 cm.

If we consider polymodal mixtures made of nearly monodisperse components, large peak capacity as well as low retention ratios are required leading to the choice of thick channels. High peak capacity associated with low particle selectivity is required, such combination is given using long an thick channels. However significant length and thickness interactions not predicted by any ''Lift-Hyperlayer'' models have been demonstrated in this study for retention ratio. The second-order response observed

for channel breadth led to the set up of broad channels. Channel set up rules for polymodal mixture are therefore made possible. From the experimental design data a thick, long and broad channel is to be preferred. However, in such a system separation can be time consuming. The channel set up strategy is therefore the following. A very thick and broad channel of moderated length is chosen in a first intention then thickness reduced. For practical use, and because of instrumental set up possibilities minimum thickness of 250 μm as well as minimum breadth of 2 cm and 50 cm long channel will be appropriate dimensions bases for G-FFF.

5. Conclusion

The experimental design methodology described in this report has formalised some effects of channel dimensions on eluted peak characteristics. The effects of each of the first-order channel dimensions were in total agreement with the results predicted by the ''Lift-Hyperlayer'' theory, particularly in the light of recent reports [32,33]. However second-order effects and interactions where revealed by the experimental design methodology, these not predicted by any model published so far. For the analyses of micron sized species, channel dimension set up is in relation with the different separation goals. It is demonstrated that different dimensions were involved as primary factor depending on the system response. The evidence of interactions between a couple of dimensions was formalised even if the physical mechanism is not established.

If a single very polydisperse population is considered, separation goal tends to separate and purify sub-populations as already shown by Cardot et al. [31]. In this case, neither a very low retention ratio nor a high peak capacity are necessary, a thin channel must be preferred, whatever its length. The consequence of this prediction is the possibility to develop miniaturised G-FFF systems. Moreover the relatively high proportion of the channel occupied by the injection volume will not compromise such a miniaturisation.

The analysis of complex mixtures made of very different but almost monodisperse constituents, requires a large peak capacity value combined with the possibility of elution at low retention ratios. Thicker channel must be preferred. However significant length and thickness interactions for retention ratio where evidenced as well as a second-order response was observed for breadth. Long, thick and broad channel should be preferred, with time consuming separations as consequence. In terms of separation development strategy the following procedure is recommended: very thick channels of moderate lengths should be preferred at first and instrumental modifications will focus on the design of thinner and thinner channels at constant void volume. One must have in mind that other parameters will play very critical roles in the separation development, channel walls characteristics as well a carrier phase composition and flow-rate.

References

[1] J.C. Giddings, P.S. Williams, Am. Lab. 25 (1993) 88.
[2] J.C. Giddings, S.K. Ratanathanawongs, M.H. Moon, KONA: Powder Particle 9 (1991) 200.
[3] J.C. Giddings, Sep. Sci. 1 (1966) 123.
[4] J.C. Giddings, Science 260 (1993) 1456.
[5] K.D. Caldwel, Y.S. Gao, Anal. Chem. 65 (1993) 1764.
[6] M. Martin, P. Reynaud, Anal. Chem. 52 (1980) 2293.
[7] M. Martin, J.C. Giddings, J. Phys. Chem. 85 (1981) 727.
[8] S.K. Ratanathanawongs, J.C. Giddings, Chromatographia 38 (1994) 545.
[9] J.C. Giddings, F.J.F. Yang, M.N. Myers, Anal. Chem. 46 (1974) 1917.
[10] J.C. Giddings, F.J.F. Yang, M.N. Myers, Sep. Sci. 10 (1975) 133.
[11] P.J.P. Cardot, C. Elga, M. Guernet, D. Godet, J.P. Andreux, J. Chromatogr B 654 (1994) 193.
[12] A. Fox, L.E. Schallinger, J.J. Kirkland, J. Microbiol. Methods 3 (1985) 273.
[13] P.S. Williams, S. Lee, J.C. Giddings, Chem. Eng. Commun. 130 (1994) 143.
[14] K.D. Caldwell, Z.Q. Cheng, P. Hradecky, J.C. Giddings, Cell Biophys. 6 (1984) 233.
[15] J.J. Kirkland, W.W. Yau, W.A. Doerner, Anal. Chem. 52 (1980) 1944.
[16] S.K. Ratanathanowongs, J.C. Giddings, Anal. Chem. 64 (1992) 6.
[17] D.J. Nagy, Anal. Chem. 61 (1989) 1934.
[18] J. Pazourek, E. Urbankova, J. Chmelik, J. Chromatogr. A 660 (1994) 113.
[19] V.R. Meyer, Practical High-Performance Liquid Chromatography, Wiley, 1988.
[20] K.D. Caldwell, S.L. Brimhall, Y. Gao, J.C. Giddings, J. Appl. Polym. Sci. 36 (1988) 703.

[21] M. Martin, A. Jaulmes, Sep. Sci. Technol. 16 (1981) 657.
[22] J.C. Giddings, Sep. Sci. 43 (1969) 181.
[23] J. Pazourek, J. Chmelik, Chromatographia 35 (1993) 591.
[24] J. Pazourek, P. Filip, F. Matulek, J. Chmelik, Sep. Sci. Technol. 28 (1993) 1859.
[25] J.J. Kirkland, W.W. Yau, W.A. Doerner, J.W. Grant, Anal. Chem. 52 (1980) 1944.
[26] M. Feinberg, La Validation des Méthodes d'Analyse, Masson, Paris, 1996.
[27] E. Assidjo, Cardot, J. Liq. Chromatogr. 20 (1997) 2579.
[28] A. Bernard, B. Paulet, V. Colin, P.J.P. Cardot, Trends Anal. Chem. 14 (1995) 266.
[29] J. Lellouch, P. Lezar, Méthodes Statistiques en Expérimentation Biologique, Flammarion, Paris, 1974.
[30] A. Lucas, F. Lepage, Ph. Cardot, in: M. Shimpf, K. Caldwell, J.C. Giddings (Eds.), Field-Flow Fractionation Handbook, Wiley–Interscience, New York, 2000, p. 471, Chapter 29.
[31] P.J.P. Cardot, M. Martin, J.M. Launay, J. Liq. Chromatogr. 20 (1997) 2543.
[32] J. Chmelik, J. Chromatogr. A 845 (1999) 285.
[33] J. Plockova, J. Chmelik, J. Chromatogr. A 868 (2000) 217.